Polymer Journal, Vol. 39, No. 9, pp. 935–944 (2007)

Amorphous-Phase Miscibility and Crystal Phases in Blends of Polymorphic Poly(hexamethylene terephthalate) with Monomorphic Poly(pentamethylene terephthalate)

Kai C. YEN, E. M. WOO,† and Yu-Fan CHEN

Department of Chemical Engineering, National Cheng Kung University, Tainan, 701, Taiwan

(Received December 20, 2006; Accepted June 9, 2007; Published July 18, 2007)

ABSTRACT: Annealing or heat scan-induced lamellar thickening and factors influencing crystal unit cells in polymorphic poly(hexamethylene terephthalate) (PHT) were probed using polarized-light optical microscopy (POM), differential scanning calorimetry (DSC), wide-angle X-ray diffraction (WAXD), synchrotron small-angle X-ray scattering (SAXS). The DSC and WAXD results show that post-scanning or annealing (up to 140 °C) on 110 °C-crystallized PHT neither transform crystal cell types nor does thin lamella into thick lamella. Rapid lamellar thickening in PHT could take place during DSC scanning, which was proven by comparing SAXS data. T_{max} (final temperature of heating); within a range of 180 up to 220 °C) does not influence the polymorphism or multiple melting peaks in PHT. All evidence suggests that kinetic factors are less influential on the polymorphism in PHT. Further, polymorphic poly(hexamethylene terephthalate) (PHT) was blended with monomorphic poly(pentamethylene terephthalate) (PPT) to form a crystalline/crystalline blend system. The semicrystalline PPT and PHT are miscible in the melt state or quenched amorphous phase. The miscibility, *via* weak intermolecular interactions, in the amorphous phase of the PHT/PPT blends exerts almost no influence on the crystalline domains, where PPT does not interfere with the formation of α or β crystal forms in PHT, and vise versa, PHT does not interfere with the sole α-crystal form in PPT. [doi:10.1295/polymj.PJ2006197]

KEY WORDS Poly(hexamethylene terephthalate) / Poly(pentamethylene terephthalate) / Miscibility /

Binary blends of two chemical-structurally similar polymers or two polymers in a homologous series have been relatively less studied in comparison to more widely-studied blends where two constituents exhibit strong or specific interactions *via* functional groups. Kwei[1,2] has reported that binary blends of poly(methyl methacrylate) (PMMA) and poly(ethyl methacrylate) (PEMA), which differ from each other by one methylene in the pendant group, are phase-separated and immiscible. However, blends of poly(benzyl methacrylate) and poly(phenyl methacrylate), which also differ from each other by one methylene in the pendant group, are single-phase and miscible.[3] A third example can be given by a poly(vinyl ether) blend system. Poly(vinyl methyl ether) and poly(vinyl ethyl ether), also differing by one methylene in pendant group, are immiscible to each other. Yet, poly(isopropyl acrylate) and poly(isopropyl methacrylate) are miscible;[4] but poly(methyl acrylate) is immiscible with poly(methyl methacrylate).[5] In addition, poly(hydroxy butyrate) (PHB) and poly(L-lactic acid) (PLLA), two widely-studied biodegradable polyesters, differ in the main-chain repeat unit only by one methylene. Nevertheless, the PHB/PLLA blend is not miscible, according to our earlier laboratory results. Thus, it may be wrong if one attempts to conclude, one way or another, about the phase behavior of a blend of two homologous polymers differing by one methylene unit in either the main chain or pendant group. Additional well-known examples of blends of two similar polymers can also be cited. A widely studied blend system of polystyrene (PS) and poly(α-methyl styrene) (PαMS) is immiscible at ambient, but exhibits a upper critical solution temperature(UCST)phenomenon at elevated temperatures.[6–12] In addition, UCST is also observed in blends of polystyrene with poly(4-methyl styrene) (P4MS).[13] However, P4MS/PαMS blend is miscible but can become phase-separated at higher temperatures with a lower critical solution temperature (LCST) phenomenon,[14] which is in contrast to the immiscibility with UCST noted for the PS/PαMS and PS/P4MS blend.

A book authored by Utracki[15] summarizes extensive thermodynamic theory backgrounds, prediction, and determination of blend miscibility. Some interesting examples as listed in the book are re-cited here to illustrate the intricacy in dealing with phase behavior in blends. Tanaka and Nishi[16–18] conducted studies on blends comprising poly(ε-caprolactone) (PCL), poly(vinyl methyl ether) (PVME), or polystyrene (PS). PS/PVME and PCL/PVME blends show LCST, while PCL/PS blend shows UCST; however, ternary blends of PS/PVME/PCL are miscible. Phase behavior in blends involving crystalline constituent(s) can

†To whom correspondence should be addressed (Tel: +886 6 275-7575 Ex. 62670, Fax: +886 6 234-4496, E-mail: emwoo@mail.ncku.edu.tw).

be influenced by an additional factor: enhancement or depression of spherulite growth rate. Martuscelli[19] reported that isotactic PS/PVME shows only partial miscibility, which is attributed to PVME enhancing the spherulite growth rate of iPS. By contrast, poly(methyl methacrylate) PMMA was observed to slow down the spherulite growth rate of poly(ethylene oxide) (PEO).[20,21] As a result, the PEO/PMMA blend is miscible. Note that these explanations based on rates have not taken into account of polymer structures, which may also be an important factor. Utracki's book provides useful guidelines for general prediction of phase behavior in blends of two dissimilar polymers; however, from the above cited examples of complex phase behavior, there seems difficulty to summarize applicable rules in predicting the phase behavior of blends of two similar polymers in a homologous series with similar chemical structures or functional groups. However, subjects of polyester/polyester blends have also attracted intensive interests lately. Miscible polyester/polyester blend systems can be illustrated with binary blends comprising any two of poly(ethylene terephthalate) (PET), poly(trimethylene terephthalate) (PTT), and poly(butylene terephthalate) (PBT) in a series of homologous aryl-polyesters.[22–27] Blends of PET and PBT were widely studied in early time:[22–24] more recently, our work has further extended to a new frontier that blends of PTT/PET and PTT/PBT are miscible.[26,27] That is, any two of the three aryl polyesters: PET, PTT, and PBT can form miscible binary blends. In addition to miscibility in binary blends, ternary blends comprising all three semicrystalline polyesters (*i.e.*, PET, PTT, and PBT) are miscible.[27] Note that these three aryl polyesters of a same functional group differ by one or two methylene units in the main chain repeat units; yet they are miscible. However, the miscibility demonstrated in blends of these polyesters does not suggest that all binary pair of polyesters of any structures will be miscible too. The structures of either of the polyester constituents in the blend may determine the phase behavior of the blend.

Poly(hexamethylene terephthalate) (PHT) and poly(pentamethylene terephthalate) (PPT) are two crystalline aryl-polyesters. They differ only by one methylene in the main-chain repeat unit; nevertheless, this difference may result in different crystallization rates, polymorphism, and spherulite morphology, or even constitute a critical factor in determining the phase behavior in blends of these two polyesters. PHT is a polymorphic polyester that has been characterized to display as many as three different crystal cells (α, β, γ) depending on thermal and/or solution treatments;[28–30] however, by contrast, PPT is packed with only a single type of crystal cell. PPT exhibits distinct banded spherulites;[31] but the PHT forms radial spherulites with Maltese-cross. Thus, it would be of great interest to probe the blends of these two polyesters, not only on phase behavior and miscibility in the amorphous phase of blends but also effect of blending on crystals, spherulites, polymorphism, etc. Effects of blending and miscibility of two crystalline polymers on polymorphism, spherulites, lamellar thickening, etc., were evaluated.

EXPERIMENTAL

Materials

Poly(hexamethylene terephthalate) (PHT) was synthesized in-house using a catalyst (butyl titanate) by following the method described earlier in the literature.[32] The weight-average molecular weight (M_w) and polydispersity index (PDI), measured by gel permeation chromatography (GPC) are 13,800 g/mol and 2.0, respectively. The melting and glass transition temperature of the synthesized PHT were characterized using a DSC, and the values are 144.3 and $-6.7\,^{\circ}C$, respectively. Note that the polymeric chains in the synthesized PHT contain at least 30 repeat units, whose characteristic crystalline morphology and melting peaks are pretty much the same as those in longer-chain PHT. Similarly, poly(pentamethylene terephthalate) (PPT) was also synthesized in-house using two-step polycondensation procedures,[31,32] by starting from *1*,*5*-pantanediol and dimethyl terephthalate with 0.1% butyl titanate as a catalyst. The molecular weight (M_w) and polydispersity index (PDI) measured by gel permeation chromatography (GPC) were 10,700 g/mol and 1.7, respectively. The melting and glass transition temperatures of the synthesized PPT were characterized using DSC to be 127.0 and $-1.3\,^{\circ}C$, respectively. By comparisons, PPT has a slightly higher T_g than PHT; but the melting point of PPT is much lower than PHT, owing to the even-odd effect known in homologous polyesters.

Apparatus

Polarized-light optical microscopy (POM). A polarized-light microscopy (Nikon Optiphot-2) equipped with charge-coupled device (CCD) digital camera, and a microscopic heating stage (Linkam THMS-600 with TP-92 temperature programmer) was used to investigate the spherulitic morphology of isothermally crystallized samples. The samples were first melted on the hot stage at $150\,^{\circ}C$ for 10 min, then quickly quenched to a designated temperature for isothermal crystallization.

Differential scanning calorimetry (DSC). DSC measurements were made in a Perkin-Elmer DSC-7 equipped with a mechanical intracooler under nitro-

gen purge. Temperature and heat flow calibrations at different heating rates were done using indium, zinc. Heating rates of 2.5, 5, 10, 20, up to 30 °C/min were used whenever needed. Melt-crystallization treatments involved that samples were first melted at 180 °C for 10 min and quickly cooled at a rate of 320 °C/min to desired isothermal temperatures (90–140 °C).

Wide-angle X-ray diffraction (WAXD). Shimadzu XRD-6000 with a copper K_α radiation ($\lambda = 0.1542$ nm) was used for WAXD measurements. The scanning 2θ angles covered a range between 5° and 35° with a step of 0.02°. For WAXD experiments, the same crystallization or annealing conditions as described in the thermal analysis section were carried out on samples that had been thermally treated in the DSC cells. It was critical to ensure that the samples for DSC and WAXD were treated exactly with the same temperature accuracies and thermal histories for comparisons.

Synchrotron small-angle X-ray scattering (SAXS). Small-angle X-ray scattering (SAXS) from a synchrotron radiation source (at National Synchrotron Research Center, Taiwan) was employed to characterize the crystalline lamellar morphology of PHT/PPT blends subjected to various thermal treatments in DSC cell to simulate the thermal scanning histories in DSC thermal analysis. SAXS experiments were performed at BL01B SWLS beamline at National Synchrotron Radiation Research Center, Taiwan. The incident X-ray beam was focused vertically by a mirror and monochromated to the energy of 10.5 keV by a silicon (111) double-crystal monochromator. The wavelength of the X-ray beam is $\lambda = 0.1181$ nm. The sample-to-detector distance is 1571 mm in length, and the beam stop is a round molybdenum disk of 4 mm in diameter. A one-dimensional position-sensitive detector (PSD) was used for collecting SAXS data, and the sensitivity of PSD was calibrated by using a ^{55}Fe source before data collection. The calibration of the detector channels in terms of scattering vector was made by linear regression over the positions of numerous orders of the long spacing of silver behenate as the standard, with $q_{max} = 1.076$ nm^{-1}. The intensity profiles were output as plots of scattering intensity (I) *vs.* scattering vector, q ($q = (4\pi/\lambda)^* \sin(\theta/2)$, where θ is the scattering angle). The standard polyethylene (PE) was used to correct SAXS data to gain the absolute intensity after subtraction of background (air scattering). All SAXS measurements were carried out at either ambient or at various higher temperatures in the hot-stage under a dry nitrogen atmosphere. The specimens of polymers or blends were placed in the sample-cell sealed by two pieces of Kapton, wherever needed. Before measuring the SAXS profile at a given temperature, 0.5 min was allowed after attaining the given temperature to ensure equilibrium. Then, the intensity distribution was accumulated for 2 min. The morphological parameters including long period (L), crystal lamellar thickness (l_c) and amorphous layer (l_a) were obtained from the one-dimensional correlation function according to the standard procedures reported in the literature.[33]

RESULTS AND DISCUSSION

Effects influencing polymorphism in PHT

PHT samples were melt-crystallized at 110 °C for 2 h to develop initial maximum crystallinity, and then heated/annealed in DSC to different intermediate temperatures (140 °C), with temperature equilibrated briefly, then quickly quenched back to 110 °C. More direct evidence for lamellar/crystal information is discussed in conjunction with wide-angle and small-angle X-ray results (WAXD and SAXS). WAXD was intended to reveal crystal units in PHT before or after thermal treatments. However, relationships between the melting peaks and lamellar morphology are yet to be exemplified for PHT. SAXS was performed to compare the lamellar morphology changes in PHT crystallized at 110 °C versus the 110 °C-crystallized PHT that was further heated 140 °C then quenched back to 110 °C. Thus, a figure of three sets of results is presented. Figure 1 shows (A) DSC traces, (B) WAXD, and (C) SAXS results of neat PHT subjected to two different thermal schemes (a and b). DSC result in Figure 1(A) is first discussed. Two sets of samples were prepared: (a) melt-crystallized PHT [110 °C, 2 h], and (b) 110 °C-crystallized PHT further scanned to 140 °C. For DSC analysis, these two set of samples were then all scanned (at identical rate of 10 °C/min) from 110 to 180 °C, in order to probe re-organization between different crystal species in PHT in relation to complex multiple melting peaks. Trace-(a) is scan for 110 °C-crystallized PHT (110 °C for 2 h), which exhibits a total sum of melting enthalpy of P_1, P_2, P_3, and $P_4 = 49.5$ J/g. Note that the highest peak (P_4) in neat PHT is actually an overlapped sum of dual peaks $P_4 + P_5$ (or P_{4+5}), which is revealed only when PHT is scanned at lower rates (5 °C/min or lower). The origin of overlapped dual peaks ($P_4 + P_5$) is beyond the scope of this article and will not be discussed here. For the scanning rate (10 °C/min) used in this study, only a single peak (P4) was revealed. For practical reason the highest peak is simply referred as P_4 (rather than P_{4+5}). In previous work, melt-crystallized PHT is already known to exhibit complex melting peaks with various states of polymorphism depending on T_c.[28–30] Here, the objective in this study was to further clarify whether post-crystallization thermal annealing/scan-

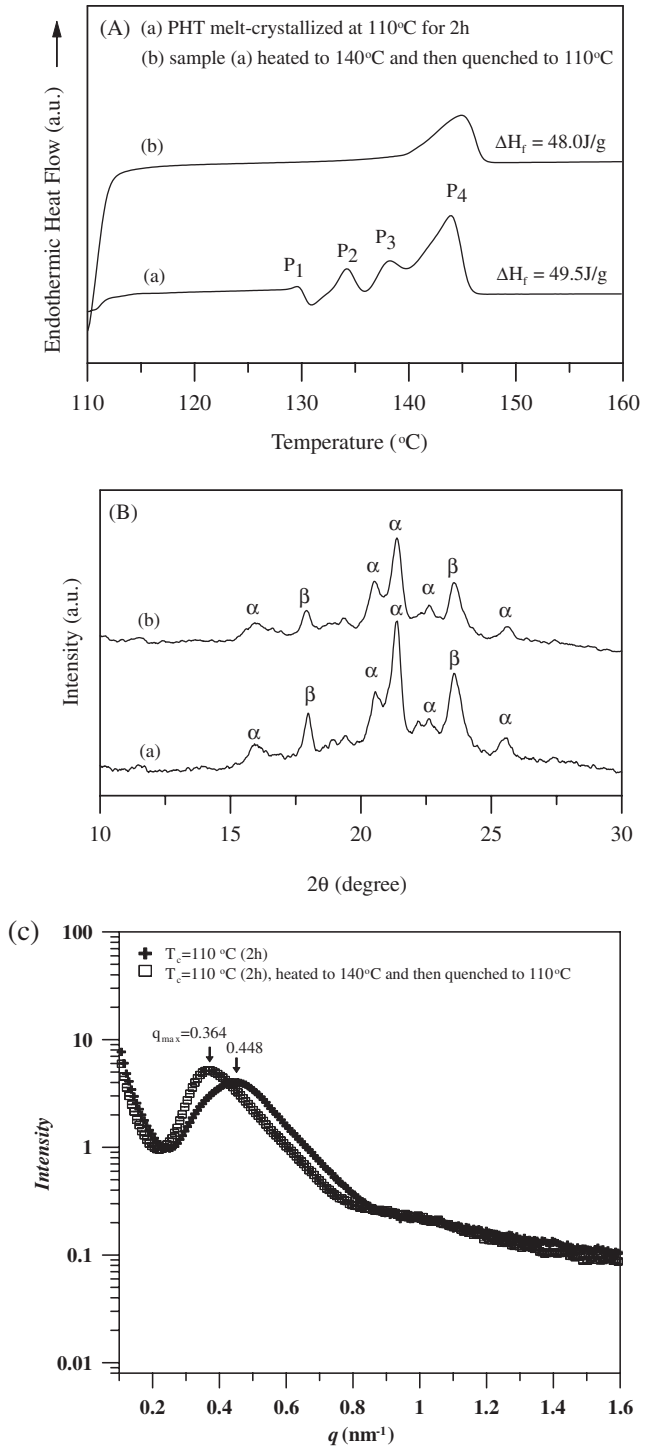

Figure 1. (A) DSC traces, (B) WAXD patterns, and (C) SAXS curves for: (a) PHT melt-crystallized at 110 °C for 2 h; (b) Sample-a annealed at 140 °C, then quenched back 110 °C.

ning at temperatures higher than the original T_c might induce polymorphism transition or lamellar thickening. Earlier work[28–30] has discussed and concluded that melting of P_1 leads to immediate re-packing into P_2 (or later P_{3+4}). Only a merged P_{3+4} peak is seen with melting/re-crystallization of P_3 at 140 °C, whose total enthalpy of melting (48 J/g) does not change much in comparison to un-annealed PHT (DSC Trace-a). Apparently, the melted species of P_3 can readily re-pack into new crystal/lamellar species of higher melting P_{3+4} at a normal scanning rate of 10 °C/min. The DSC results show that the heating scan in DSC induces almost immediate re-packing of melted species into new lamellar crystals, and scan-induced thickening of lamellae takes place in multiple (as many as four) steps for PHT within a narrow temperature range. It would be of interest to compare the melting peak of a 140 °C-melt-crystallized PHT[30] with that of 110 °C-melt-crystallized PHT then post-scanned to 140 °C, as shown in DSC Trace-b of this figure. DSC melting peaks of the former (140 °C-melt crystallized PHT) is sharper and narrower[30] than the latter (110 °C-melt-crystallized then heat-scanned to 140 °C). Thus, the DSC result seems to suggest that post-scanning or annealing (up to 140 °C) on the 110 °C-crystallized PHT sample does not completely and uniformly transform all thin lamella into thick lamella.

Figure 1(B) (curves-a and b) shows the corresponding WAXD patterns: (a) PHT melt-crystallized at 110 °C for 2 h; (b) Sample-a annealed at 132 °C then quenched back to 110 °C; (c) Sample-a annealed at 136 °C, then quench back 110 °C; (d) Sample-a annealed at 140 °C, then quenched back 110 °C. The result shows the same diffraction peaks, indicating that these PHT samples, having been subjected to different annealing schemes, all contain the same α and β crystal forms regardless of melting and re-organization of P_1, P_2, or P_{3+4}. New lamellar species of P_{3+4} is formed *via* re-organization upon melting of initial P_1, P_2, or P_{3+4} crystals, but the crystal cells are similar in containing both α and β cells. Post-scanning (or annealing) to 140 °C on the 110 °C-crystallized PHT sample only diminished the fraction of α-crystal, by judging from the relative peak intensity; but did not completely transform all initial α-crystal to β-crystal. Note that if PHT is directly melt-crystallized at the high $T_c = 140$ °C (for up to 24 h), the β crystal would be the sole crystal species in PHT and at this temperature it tends to pack into large dendritic spherulites instead of regular Maltese-cross spherulites.[30] Furthermore, changes in lamellar thickness were characterized using SAXS. Figure 1(C) (Curves-a, b) shows SAXS curves for (a) PHT crystallized at $T_c = 110$ °C, and (b) PHT crystallized at $T_c = 110$ °C (2 h), heated to 140 °C, then quenched to 110 °C. Result is summarized as following: (a) $q_{max} = 0.448\,nm^{-1}$, long period = 14.0 nm; (b) $q_{max} = 0.364\,nm^{-1}$, long period = 17.2 nm, where q_{max} is defined as the q value which corresponded to the highest intensity of the peak and the higher intensity might be due to the fluctuation not related to the spacing of the lamellae and amorphous. Here, we only intend to compare the peak

positions and not absolute scale of intensity; therefore, curves are plotted in offset scale. The relationship between the long period and lamellar thickness can be described by $l_c = L^* \phi_c^{line}$ by similar treatments as described in a previous work,[34] where l_c is the lamellar thickness, L is the long period and ϕ_c^{line} is linear crystallinity. Besides, ϕ_c^{line} is defined as the ratio of ϕ_c/ϕ^s, in which ϕ_c is the bulk crystallinity obtained from DSC or WAXD and ϕ^s is the volume fraction filled with the lamellar stacks which can be obtained from POM observation of the fraction of the spherulites. If there is no domain between the spherulites, ϕ^s can be taken as 1. In this study, ϕ^s was taken as 1.0 for both PHT samples were densely and fully filled with spherulites. Thus, the lamellar thickness is proportional to the product of bulk crystallinity and long period. Moreover, the bulk crystallinity can be calculated from the ratio of $\Delta H_f/\Delta H_f^o$, in which ΔH_f^o for these two samples is equal and the values of ΔH_f are almost same. Thus, it can be concluded that thickening of lamella takes place in the PHT sample crystallized at $T_c = 110\,^\circ C$ (2 h), scan-heated to 140 °C (in DSC at 10 °C/min) then quickly quenched back to 110 °C. The SAXS result further proves that the multiple melting peaks are attributed to melting/re-crystallization/re-melting to thicker lamella, and not to polymorphism of PHT. Both SAXS curves possess a distribution, but the distribution is relatively narrower for the PHT with post-scanning to 140 °C. In addition, the SAXS curve for the PHT with post-scanning to 140 °C clearly shifts to a lower q value, and the fractions with lower q values are apparently greater, indicating that lamellar species are thickened.

For PHT, it was of interest to clarify whether T_{max} (temperature for melting the crystals) might influence the polymorphism. Some crystalline polymers with polymorphism, such as syndiotactic polystyrene (sPS), is known to exhibit a specific preference for crystal cells sensitive to T_{max} from which the melt is kept prior to being quenched to a designated T_c for crystallization. T_{max} between 180 to 220 °C were selected in this study since dependence of the lamellar thickness on ΔT in α form may be different from β form. Influence of T_{max} on polymorphic nature and crystal cells in PHT was also investigated. PHT crystallized between 90, 120, and 130 °C has been known to display polymorphism of α and β form crystals. Figure 2 shows WAXD diffractograms of PHT samples crystallized at various temperatures (90, 120, 130 °C) by quenching from the melt at $T_{max} = 180$ or 200 °C. The characteristic peak of α form (*i.e.*, $2\theta = 15.9°$, $20.5°$, $21.2°$, $25.4°$) and β form (*i.e.*, $2\theta = 17.9°$, $23.6°$) are clearly observed regardless of T_{max}. By quenching from the melt at either $T_{max} =$ 180 or 200 °C, PHT displays the same α and β form

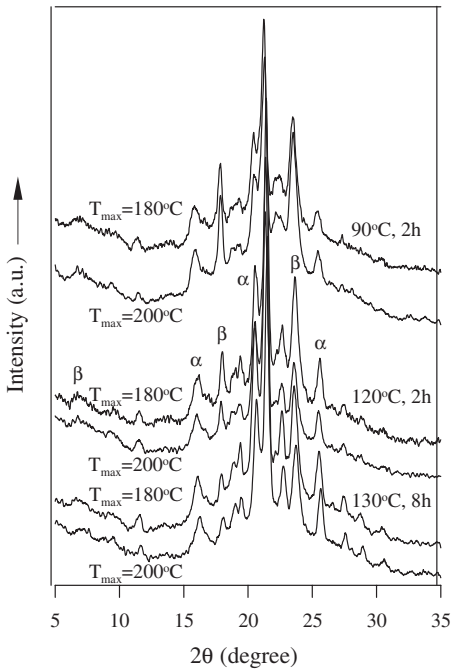

Figure 2. WAXD patterns of PHT melt-crystallized at 90, 120, 130 °C, respectively, after quenching from $T_{max} = 180\,^\circ C$ or 200 °C.

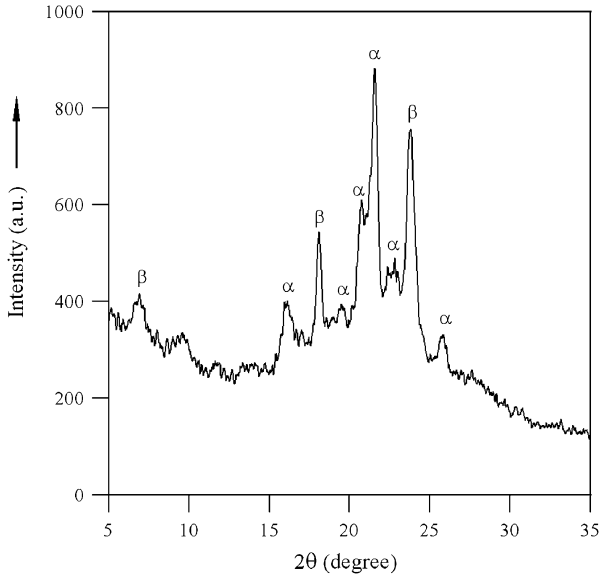

Figure 3. WAXD patterns of PHT melt-crystallized at 110 °C, after quenching from $T_{max} = 220\,^\circ C$.

crystals. Effect of higher T_{max} was also analyzed. Figure 3 shows WAXD result of PHT crystallized at 110 °C (1 h) after quenching from $T_{max} = 220\,^\circ C$ (5 min). The WAXD diffractogram shows dual cells in crystal packing similar to the polymorphism in PHT subjected to lower T_{max}, indicating that T_{max} (between 180–220 °C) had virtually no effects on alternating the polymorphic crystal cells. By increasing T_{max} to this higher temperature (220 °C), the WAXD analysis apparently reveals the same result as those

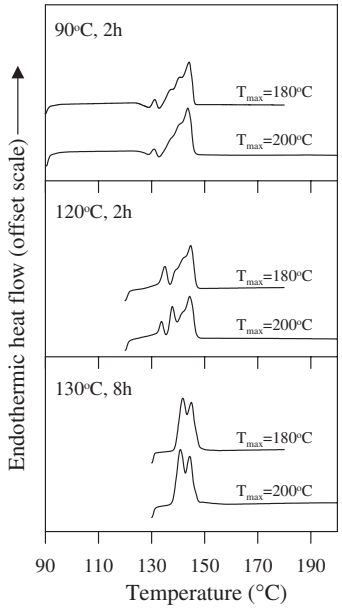

Figure 4. DSC traces (scan rate: 10 °C/min) for PHT crystallized at 90, 120, or 130 °C, after quenching from melt at T_{max} = 180 or 200 °C.

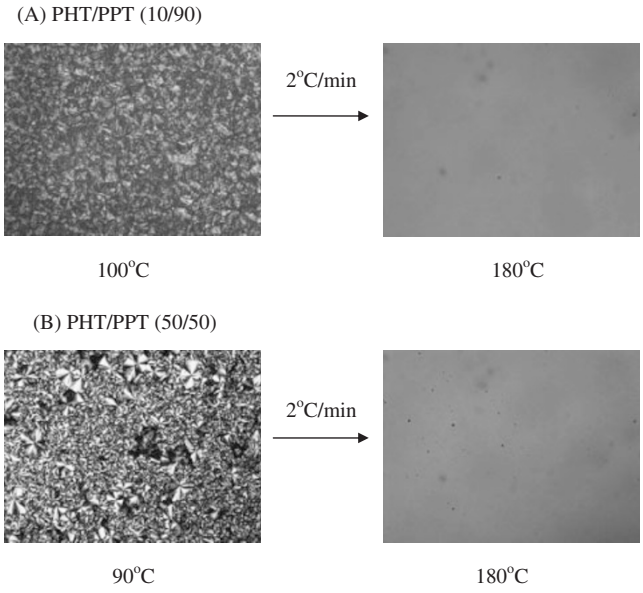

Figure 5. POM graphs of PHT/PPT blends (10/90 and 50/50) below or above melting point.

for lower T_{max} imposed on PHT. This result of polymorphism independent of T_{max} for PHT is quite different from that found for other polymorphic polymer, *e.g.*, syndiotactic polystyrene. For syndiotactic polystyrene (sPS), the maximum temperature (T_{max}) from which the polymer is quenched to melt-crystallization has been found to be a critical factor in determining the crystal cell types and polymorphism.[35,36]

In addition, DSC characterization was performed to evaluate effects of T_{max} on the thermal behavior and lamellar crystal species in PHT. For direct comparisons, the thermal schemes on the DSC samples corresponded exactly to those on the samples used in WAXD characterization.

Figure 4 shows DSC traces of PHT samples crystallized at various temperatures (90, 120, and 130 °C, respectively) by quenching from the melt held 5 min at T_{max} = 180 or 200 °C, respectively. The DSC result shows that the melting behavior of PHT crystallized from melt at either high-T_{max} (200 °C) low-T_{max} (180 °C) is almost identical, suggesting that T_{max} has no influence on the crystalline lamellae and their related thermal transitions in PHT. Note that minor difference in DSC melting curves for blends at T_c = 120 °C is seen, which might have been caused by minor thermal history difference in the samples (one being quenched from T_{max} = 200 °C while the other from T_{max} = 180 °C.) But overall, this minor difference in DSC curves does not negate the broader observation that T_{max} has no influence on polymorphism, which has been extracted from evidence in bother X-ray analysis and DSC curves.

Miscibility in PHT/PPT blend

Effect of amorphous-phase miscibility on crystal polymorphism in PHT was also probed. Miscibility of the PHT/PPT blends was investigated by OM and DSC characterizations. Figure 5 shows OM micrographs for the PHT/PPT blends, which clearly reveal that all blends are homogeneous in the melt, with one-phase morphology and free of any discernible phase domains. Thermal analysis was also performed. Figure 6 shows the DSC curves (20 °C/min) for the PHT/PPT blends of various PPT contents. All blend samples were heated to melt and rapidly quenched to −30 °C to an amorphous state prior to initiation of DSC scanning. Although the proximity of T_g's of PHT and PPT makes it difficult to discern, there is clearly only one single and composition-dependent T_g (marked with arrow) for each of the blend compositions. Note that for the PHT/PPT (50/50) blend, there are two apparent cold crystallization endotherm peaks, with the first one being associated with PHT and the second one with PPT species. The fact indicates that each of two crystallizing species in the blends crystallizes into distinct and separate crystalline domains. The DSC traces show that, for most other blend compositions, there is only one cold-crystallization endotherm, whose peak temperature varies with the composition. The cold-crystallization temperature of PHT apparently increases with increasing PPT contents, which suggests that the PHT polymer chain mobility in the blends is influenced by its interactions with PPT. The higher-T_g PPT species, through interactions with PHT chains, makes PHT slightly more rigid than neat PHT at the same T_c; thus, at

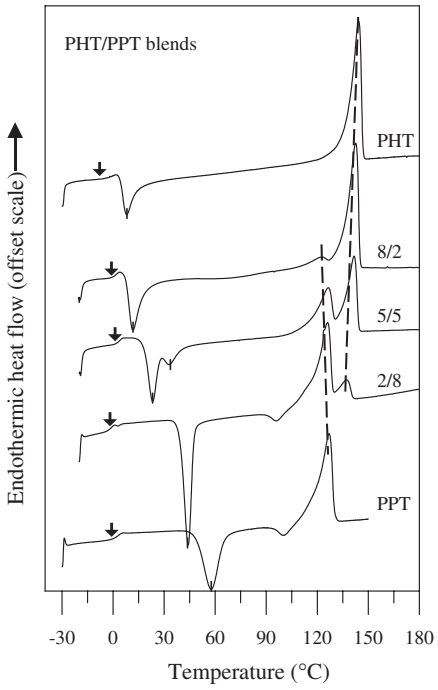

Figure 6. DSC curves showing single T_g for PHT/PPT blends of different compositions.

increasing PPT contents in the PHT/PPT blends, T_c at which PHT cold crystallization (during scanning) occurs at increasingly higher temperatures and merges with the cold crystallization of PPT. Besides, for the PHT-rich blend (PHT/PPT = 80/20) there was only one cold-crystallization peak, because the crystallization rate of PHT is higher than PPT and the amount of PPT was relatively low, thus the cold-crystallization of PPT might be suppressed.

In addition to the change of the cold-crystallization temperatures ($T_{c.c}$) as discussed, shift of glass transition temperatures and melting temperatures of two components in blends with respect to PHT content were determined and the results were plotted. Figure 7(A) and (B) shows (A) variation of T_g of blend, and (B) depression of T_m's of PHT and PPT in blends. Figure 7(A) shows the composition dependence of T_g. Apparently, T_g's of blends vary with respect to composition; hoween, owing to proximity of T_g of PHT and PPT, scattering of data is superimposed on the variation trend. Figure 7(B) shows the depression of the melting temperature of PHT and PPT with respect to the increase of PHT constituent. For both PTT and PHT in blends, depression of T_m of one constituent in presence of the other is quite apparent. All thermal and morphology evidence as discussed above clearly shows that the PHT/PPT blend is a truly miscible binary blend system (in melt state or amorphous phase).

Effect of blend miscibility in PHT/PPT on crystal forms in PHT was evaluated. Figure 8 shows the

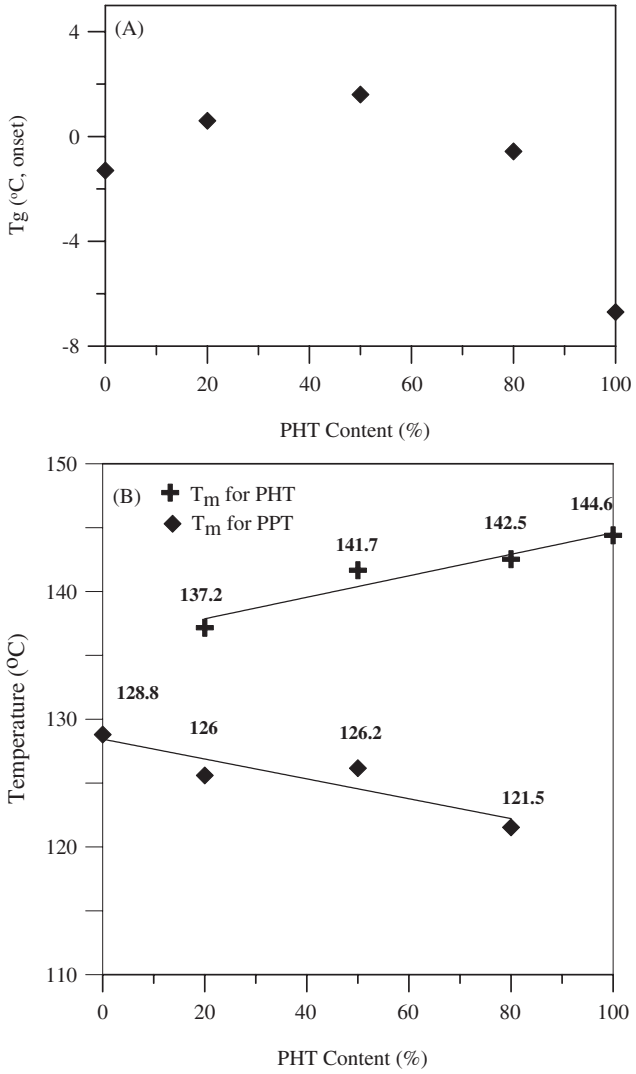

Figure 7. Composition dependence of (A) T_g (onset) and (B) T_m of PPT and PHT in PHT/PPT blends.

DSC curves of neat PHT, neat PPT, and PHT/PPT blends (compositions: 2/8, 5/5, 8/2 in wt. ratio) subjected to crystallization at 120 °C for 30 min from the melt. The temperature of $T_c = 120$ °C was selected since it was close to the melting temperature of PPT (*e.g.* 127 °C), at which PPT crystallization was retarded and the PPT constituent in the blend remained amorphous within 30 min of time after quenching from melt to 120 °C. The DSC traces in this figure show that the PHT/PPT blends exhibit similar multiple melting peaks as those seen in neat PHT. Previous work has demonstrated assignments of four multiple melting peaks in neat PHT.[30] For comparison, the DSC trace showing four melting peaks (*i.e.* P_1, P_2, P_3, P_4) is shown again for the neat PHT melt-crystallized at 120 °C for 30 min. All four melting peaks in neat PHT are clearly and well resolved. The DSC traces for the PHT/PPT blend, however, show three peaks, which are P_1, P_2, and an overlapped $P_3 + P_4$ peak. For the blend, P_1 and P_2 peaks can be partially

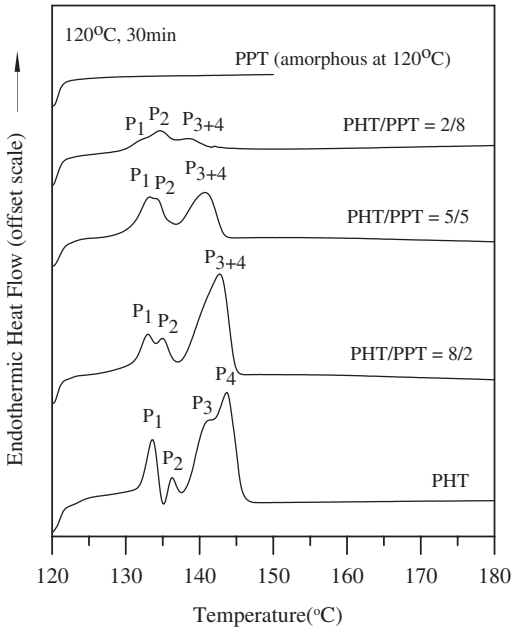

Figure 8. DSC traces showing multiple melting peaks in PHT/PPT blends (compositions: 2/8, 5/5, 8/2) in comparison with those in neat PHT, all crystallized at 120 °C for 30 min from melt.

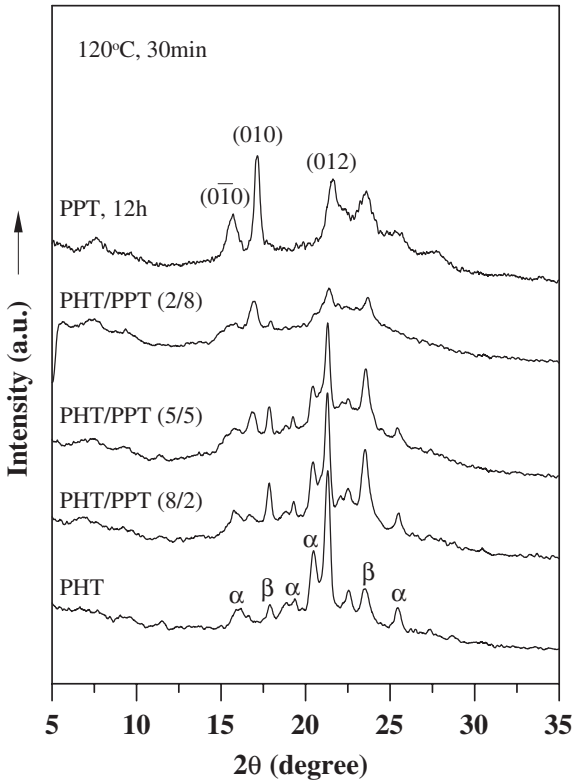

Figure 9. WAXD patterns for neat PHT in comparison with PHT/PPT blends (compositions: 2/8, 5/5, 8/2 in wt. ratios) crystallized at 120 °C for 30 min after quenching from melt.

overlapped, too. Apparently, presence of the miscible PPT (remaining amorphous/liquid) constituent in the blend influences to different degrees the lamellar species of $P_1 \sim P_4$ in PHT. The lamellar species of P_1 in PHT seems to be the most disturbed with increasing PPT in the blends. Note that the PPT constituent in blends, as well as the neat PPT, remains amorphous upon crystallization at 120 °C for 30 min; thus, the only crystallizing species in the blends is only the PHT constituent under the crystallization condition. All melting peaks for the blends are related to the lamellar crystals of the PHT component.

WAXD was performed on the blend samples corresponding to those in Figure 8 in order to correlate crystal forms with the thermal behavior in PPT/PHT blends. Figure 9 shows WAXD patterns for PHT/PPT blends (compositions: 2/8, 5/5, 8/2 in wt. ratio) subjected to crystallization at 120 °C for 30 min after quenching from melt. Note that PPT in the blend is and remains amorphous at 120 °C when held *in-situ* in DSC cell. However, the WAXD experiments on PHT or PHT/PPT blend were not performed *in situ* at 120 °C. All WAXD samples were thermally treated as described, but then quenched back to ambient, removed from DSC cell, then placed on WAXD sample holder to X-ray analysis. Thus, PPT at ambient temperature can develop some crystallinity, which is seen in the diffractogram for PPT. This difference does not influence intended analysis. The WAXD result shows that dual α and β crystal forms characteristic of PHT are present in the PHT/PPT blends. For the blends with high PPT contents, the PHT and PPT constituents both are capable of forming individual crystal species. Marks are indicated for identifying some of the unit-cell diffraction planes for the α-form crystal in the neat PPT.[31] Apparently, a few peaks of unit-cell diffraction planes in the PPT constituent may be overlapping with those from PHT in blends, but other distinct and separate diffraction peaks in the PPT constituent also present to distinguish from those of PHT. Thus, the polymorphism of the PHT constituent in the miscible blend state is almost identical to that of the neat PHT, except that the blends also display additional characteristic diffraction peaks of the PPT component. Thus, the WAXD data prove that separate PHT and PPT crystal cells exist independently, rather than co-crystallize into a new common crystal unit, in the PHT/PPT blends. Addition of PPT in the blend does not interfere with the formation of α or β crystal forms in PHT; vise versa, PHT does not interfere with the α-crystal forms in PPT. The crystal forms (unit cells) and spherulites in the PPT/PHT blends are not affected by the presence of the other species. However, discrete/separate unit crystal cells do not necessarily mean that the lamellae or spherulites are separate in the PHT/PPT blends. The PPT and PHT lamellae, each being packed with different unit cells, can still grow jointly within a same spherulite. Thus, it cannot

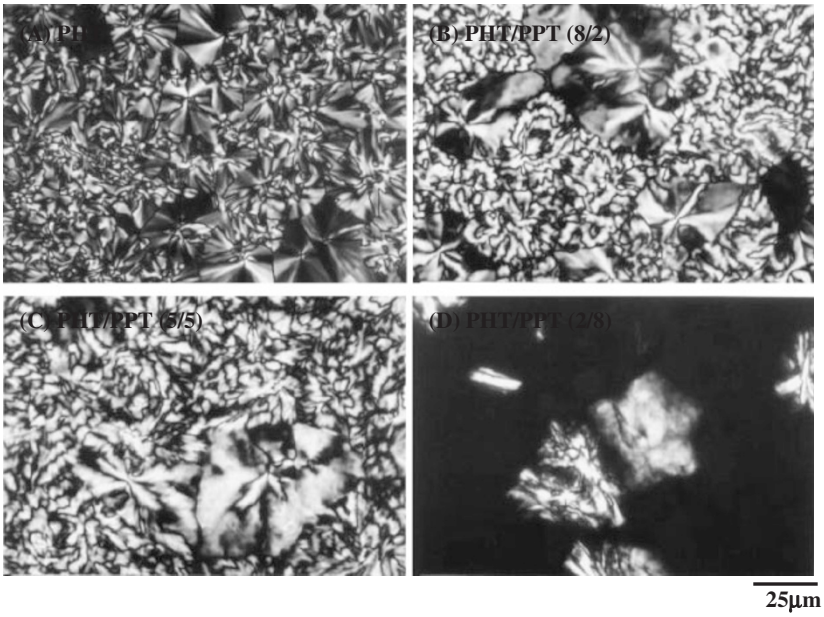

Figure 10. POM micrographs of PHT/PPT blends: (A) neat PHT, and blend compositions of: (B) 8/2, (C) 5/5, and (D) 2/8. Samples crystallized at 120 °C for 30 min after quenching from melt.

be ruled out that lamellae of both types might still integrate into common bundles that grow simultaneously and pack in a same spherulite.

Figure 10 shows spherulitic patterns in neat PHT and PHT/PPT blends. The spherulitic morphology of the PHT/PPT blends with high PHT contents is almost identical to that of neat PHT. Incorporation of PPT in PHT tends to decrease the crystallization rate, size of spherulites, and crystallinity of PHT in blends. The spherulites in the PPT/PHT blends are not affected by the presence of the other species. The sizes and patterns of spherulites in the PHT/PPT blends bear similarity with those in neat PHT or PPT, indicating that the PHT or PPT species each crystallizes individually from a homogeneous liquid mixture of PHT/PPT blend. The crystallinity in the blend is lower than that in neat PHT crystallized in similar conditions, and the PHT/PPT blends with high PPT contents (80% PPT) are not readily crystallizable when kept at 120 °C for 30 min. Neat PPT by itself possesses lower crystallizability; therefore, the crystallizability of the PPT constituent in PHT/PPT blends is even more depressed, owing to blend miscibility and interactions between PHT and PPT.

CONCLUSION

DSC result shows that post-scanning or annealing (up to 140 °C) on 110 °C-crystallized PHT sample does not completely and uniformly transform all thin lamella into thick lamella. The WAXD result shows that post-scanning or annealing (up to 140 °C) does not completely and uniformly transform all thin lamella into thick lamella, nor does it completely transform all original $\alpha + \beta$ crystal cells into sole β-cell species. Lamellar thickening during scanning is proven for PHT by comparing SAXS data for one being crystallized only at $T_c = 110$ °C (2 h) with the other being crystallized at $T_c = 110$ °C then scan-heated to 140 °C (in DSC at 10 °C/min) and quickly quenched back to 110 °C. Both SAXS curves possess a distribution, but the distribution is relatively narrower for the PHT with post-scanning to 140 °C. In addition, the SAXS curve for the PHT with post-scanning to 140 °C clearly shifts to a lower q value, and the fractions with lower q values are apparently greater, indicating that lamellar species are thickened. Melt kept at T_{max} (within a range of 180 to 220 °C) does not influence the polymorphism or multiple melting peaks in PHT. The significant factor that influences the polymorphism in PHT is the temperature, but not the crystallization time. Crystallization modes from a quenched glass or liquid melt does not seem to alter the polymorphism in PHT either. That is, kinetic factors are not influential on the polymorphism in PHT.

The PHT/PPT blend is proven to be a miscible crystalline/crystalline blend (in the melt state or quenched amorphous phase). Effect of blend miscibility on complex crystal forms and melting peaks in PHT was further evaluated. The miscibility, *via* weak intermolecular interactions, in the amorphous phase of the PHT/PPT blends exerts only limited influence on the crystalline domains. Most crystalline characteristics of either component (PHT and PPT) in blends remain unchanged. Polymorphism and multiple melting

behavior of PHT in blends are similar to neat PHT. PPT does not interfere with the formation of α or β crystal forms in PHT, and vise versa, PHT does not interfere with the α-crystal forms in PPT. The crystalline phases in the crystalline/crystalline PHT/PPT blend are distinct with separate crystals of PHT and PPT, respectively, and no evidence shows co-crystallization of both PHT and PPT chains in a common unit cell.

Acknowledgment. This work was financially supported by a basic research grant (NSC-94 2216 E006 003) in three consecutive years from *National Science Council* (NSC) of Taiwan. Beam-line at National Synchrotron Radiation Research Center, Taiwan, and staff assistance therein for helping perform the SAXS experiments are highly appreciated.

REFERENCES

1. T. K. Kwei, H. L. Frisch, W. Radigan, and S. Vogel, *Macromolecules*, **10**, 157 (1977).
2. T. K. Kwei, H. L. Frisch, W. Radigan, and S. Vogel, *Am. Chem. Soc. Div. Org. Coat. Plast. Chem. Pap.*, **37(1)**, 116 (1977).
3. S. C. Lee and E. M. Woo, *J. Polym. Sci., Part B: Polym. Phys.*, **40**, 747 (2002).
4. S. Krause and N. Roman, *J. Polym. Sci., Part A: Polym. Chem.*, **3**, 1631 (1965).
5. S. Krause, *J. Macromol. Sci., Rev. Macromol. Chem.*, **7**, 251 (1972).
6. S. Saeki, J. M. G. Cowie, and I. McEwen, *Polymer*, **24**, 60 (1983).
7. J. M. G. Cowie and I. McEwen, *Polymer*, **26**, 1662 (1985).
8. J. M. Widmaier and G. Mignard, *Eur. Polym. J.*, **23**, 989 (1987).
9. J. L. Lin and R. J. Roe, *Macromolecules*, **20**, 218 (1987).
10. H. A. Schneider and P. Dilger, *Polym. Bull.*, **21**, 265 (1989).
11. A. Rameau, Y. Gallot, B. Marie, and P. Farnoux, *Polymer*, **30**, 386 (1989).
12. T. A. Callaghan and D. R. Paul, *Macromolecules*, **26**, 2439 (1993).
13. L. L. Chang and E. M. Woo, *Macromol. Chem. Phys.*, **202**, 636 (2001).
14. L. L. Chang and E. M. Woo, *Macromolecules*, **33**, 6892 (2000).
15. L. A. Utracki, in "Polymer Alloys and Blends," Part 2, Hanser, New York, 1989.
16. H. Tanaka and T. Nishi, *J. Appl. Phys.*, **59**, 1488 (1986).
17. H. Tanaka and T. Nishi, *J. Fac. Eng. Univ. Tokyo*, **A-21**, 36 (1983).
18. H. Tanaka, T. Ikeda, and T. Nishi, *Appl. Phys. Lett.*, **48**, 393 (1986).
19. E. Martuscelli, C. Sellitti, and C. Silvestre, *Makromol. Chem., Rapid Commun.*, **6**, 125 (1985).
20. M. L. Addonizio, E. Martuscelli, and C. Silvestre, *Polymer*, **28**, 183 (1987).
21. Z. Bartczak and E. Martuscelli, *Makromol. Chem.*, **188**, 445 (1987).
22. I. Avramov and N. Avramova, *J. Macromol. Sci., Phys.*, **B30**, 335 (1991).
23. N. Avramova, S. Fakirov, and I. Avramov, *Die Angew. Makromol. Chem.*, **199**, 129 (1992).
24. S. Fakirov, M. Evstatiev, and S. Petrovich, *Macromolecules*, **26**, 5219 (1993).
25. N. Avramova, *Polymer*, **36**, 801 (1995).
26. Y. H. Kuo and E. M. Woo, *Polym. J.*, **35**, 236 (2003).
27. Y. H. Kuo and E. M. Woo, *J. Polym. Sci., Part B: Polym. Phys.*, **41**, 2349 (2003).
28. I. H. Hall and B. A. Ibrahim, *Polymer*, **20**, 783, (1982).
29. A. Palmer, S. Poulin-Dandur, J. F. Revol, and F. Brisse, *Eur. Polym. J.*, **20**, 783 (1984).
30. E. M. Woo, P. L. Wu, C. P. Chiang, and H. L. Liu, *Macromol. Chem., Rapid Commun.*, **25**, 942 (2004).
31. P. L. Wu, E. M. Woo, and H. L. Liu, *J. Polym. Sci., Part B: Polym. Phys.*, **42**, 4421 (2004).
32. M. Gilbert and F. Hybart, *Polymer*, **13**, 327 (1972).
33. G. R. Strobl and M. Schneider, *J. Polym. Sci., Part B: Polym. Phys.*, **18**, 1343 (1980).
34. W. P. Liao, T. L. Lin, E. M. Woo, and C. Wang, *J. Polym. Res.*, **9**, 91 (2002).
35. R. M. Ho, C. P. Lin, H. Y. Tsai, and E. M. Woo, *Macromolecules*, **33**, 6517 (2000).
36. E. M. Woo, Y. S. Sun, and C. P. Yang, *Prog. Polym. Sci.*, **26**, 945 (2001).